ELSEVIER

International Journal of Mass Spectrometry 204 (2001) 171–183

International Journal of Mass Spectrometry

Reactions of multidentate ligands with ligated alkali cation complexes: self-exchange and "sandwich" complex formation kinetics of gas phase crown ether–alkali cation complexes

Jeremy B. Nicoll, David V. Dearden*

Department of Chemistry and Biochemistry, C100 Benson Science Building, Brigham Young University, Provo, Utah 84602-5700, USA

Received 12 June 2000, accepted 3 July 2000

Abstract

Natural abundance isotopic labeling has been employed to study the reactions of labeled LM^+ complexes with L (L = triglyme, TG; 12-crown-4, C4; 15-crown-5, C5; 18-crown-6, C6; or 21-crown-7, C7; M = Li, Na, K, Rb, or Cs) in the gas phase using Fourier transform ion cyclotron resonance mass spectrometry. Reaction efficiencies for both ligand exchange and the formation of 2:1 ligand:metal "sandwich" complexes were determined. For a given ligand, self-exchange rates generally decrease with increasing metal size, while the sandwich complex formation rates show strong dependence on the relative sizes of the metal ions and ligand cavities. Acyclic TG complexes undergo self-exchange more rapidly than the analogous cyclic C4 complexes, whereas the sandwich complex formation rates are faster for the C4 complexes. Sandwich formation rates show a weak positive pressure dependence, as increased pressure leads to increased collisional stabilization of the complexes. Extrapolation of the rates to the zero pressure limits still yields significant rates, reflecting radiative stabilization. The self-exchange reactions have weak, negative pressure dependences, suggesting they are in direct competition with sandwich complex formation. Analysis of the sandwich complex formation radiative association kinetics yields estimates of binding enthalpies for attachment of the second ligand. Trends in the binding enthalpies, like the kinetics, show strong dependence on the relative sizes of the metal ions and ligand cavities. For a given metal, binding of a second TG is weaker than binding of a second C4. Binding enthalpies for the second ligand are in every case substantially less than calculated binding enthalpies for the first ligand to attach to a given metal. (Int J Mass Spectrom 204 (2001) 171–183) © 2001 Elsevier Science B.V.

Keywords: Crown ether; Alkali cation; Kinetics; Ligand exchange; Radiative association

1. Introduction

The examination of molecular recognition in the gas phase, in the absence of the complicating effects that arise due to solvation or the presence of counter-ions, is receiving increasing attention both within and beyond the ion–molecule chemistry community. Molecular recognition has been studied for a number of cyclic and bicyclic ligands both in the gas phase [1] and in solution [2]. Such studies have typically investigated such issues as size effects, substituent effects, and chiral recognition.

Gas phase kinetic experiments with crown ethers have examined the rates of alkali cation transfer between ligands with cavities of different sizes and

* Corresponding author. E-mail: david_dearden@byu.edu

PII S1387-3806(00)00329-8

different cation affinities [3–10], and between substituted crowns with cavities of similar size but different cation affinities [11,12]. The patterns in the rate constants as the metals are varied suggest the size relationship between the crown cavities and the metal cation is important in determining the transfer rates, but this conclusion is ambiguous because the differences in cation affinities or ligand cavity sizes can mask the subtle effects expected from cation-cavity size relationships alone.

A way to eliminate such complicating effects is to examine rates for thermoneutral exchange between isotopically labeled ligands with identical cavity sizes, for a series of cations of varying size. With the ion isolation abilities inherent in Fourier transform ion cyclotron resonance/mass spectrometry (FTICR/MS) [13], isolation of one isotopomer of a complex and observation of the reappearance of the other as a function of time can be used to measure rate constants for self-exchange, or exchange of an ion between essentially identical ligands. Extraction of the rate constants for self-exchange from these experiments can therefore be used to elucidate characteristics of the intrinsic binding affinity in the absence of enthalpic driving forces.

In this article we report rates of self-exchange (transfer of metal ion from a labeled ligand to an identical ligand) and sandwich formation (adduction of two ligands onto one metal ion), for a series of crown ethers and triglyme (triethylene glycol dimethyl ether) reacting with a series of alkali metal ions. The results can be understood in terms of the relative sizes of the cations and ligand cavities. In addition, we analyze the sandwich formation kinetics using a simple radiative association model [14] to estimate binding enthalpies for adding a second ligand to the alkali cation–ligand complexes.

2. Experimental

All experiments used a FTICR/MS (model Apex 47e, Bruker Daltonics; Billerica, MA) with a 4.7 Tesla superconducting magnet. Because the reaction involves a self-exchange, the reactants must be labeled to distinguish them from the products. This was accomplished by natural abundance isotope labeling (NAIL). NAIL involves isolation of the M+1 peak arising from the presence of naturally occurring ^{13}C among the atoms of the ligand. For a molecule such as 18-crown-6 (C6), which contains 12 carbon atoms, the M+1 peak is relatively intense (13.2% of the all-^{12}C peak), facilitating easy isolation. The M+1 (^{13}C) peak was isolated using a home-built implementation of the stored waveform inverse Fourier transform (SWIFT) [15] technique to minimize translational heating during the isolation process [16].

To study the rates of self-exchange, NAIL experiments were performed with the complexes of the ligands 12-crown-4 (C4; Aldrich), triglyme (triethylene glycol dimethyl ether, an acyclic C4 analog, hereafter denoted as TG; Aldrich), 15-crown-5 (C5; Parish Chemical; Orem, UT), 18-crown-6 (C6; Parish), and 21-crown-7 (C7; Parish) with the alkali metal ions Li^+, Na^+, K^+, Rb^+, and Cs^+. Typically, three or more metals were studied concurrently to assure that the neutral pressure was identical for each. Therefore, although the absolute errors in the measured reaction efficiencies may be large due to uncertainties in the measurement of neutral pressures and inaccuracy in calculating the collision rates, the relative values for the various metal ions with a given ligand are probably correct to the level of the reproducibility of the data. Solutions containing one crown ether and a mixture of the alkali metals were prepared and electrosprayed. Typical concentrations were 2 mM in ligand and 4 mM total in alkali metals in 50:50 methanol: water. Ratios of alkali metal concentrations were adjusted to yield approximately equal signal intensities of adduct peaks after isolation.

Neutral crown ether or glyme was introduced into the trapping cell region either by using a direct-exposure solid sample vacuum lock for samples with low vapor pressures (C6, C7), or by way of precision variable leak valves (Varian, Palo Alto, CA), after multiple freeze-pump-thaw cycles, for samples of higher volatility (TG, C4, C5). The pressure of the neutrals was monitored with a magnetically shielded cold cathode gauge (model IKR050, Balzers) located about 70 cm away from the ion-trapping cell and

immediately above the final stage cryopump (Edwards). Cell pressures were also estimated by examining the rate of transient signal decay.

After isolation of the M+1 peak, the reappearance of the M (all-^{12}C) peak was monitored over time. The peak intensities were normalized to the sum of all species with which a given peak is connected by reaction. The rates of self-exchange (exchange of the labeled ligand for unlabeled ligand) were extracted from the data using a kinetics fitting routine (KINFIT) that numerically solves a system of coupled ordinary differential equations using the Adams algorithm [17] and fits the numerical solution to the experimental data using the Marquardt algorithm. In many cases, sandwich formation (involving complexation of two ligands with one metal) was observed to compete with self-exchange, complicating the solution of the differential equations.

Variable pressure experiments with C4 self-exchange were performed by maintaining a constant pressure of C4 in the ion trapping cell region, and varying the pressure of added N_2. Rate constants were extracted for reactions of Na^+, Rb^+, and Cs^+ ions with C4, and the rate constants were extrapolated linearly to the zero pressure limit.

Conformational searches for L_2M^+ complexes, L = TG, C4, C5, or C6; M = Li^+, Na^+, K^+, Rb^+, or Cs^+ were carried out using the Monte Carlo algorithms implemented in MacroModel, version 6.5 (Schrödinger, Inc.; Portland, OR). The AMBER* force field supplied with MacroModel was used to describe interactions in the complexes. Typically, 10 000 starting geometries were used in the conformational searches.

Semi-empirical PM3 [18,19] calculations for a few of the complexes were carried out using the SPARTAN modeling package, version 5.0 (Wavefunction, Inc.; Irvine, CA). PM3 was used to minimize the structures of the complexes of Li^+ with each of the crown ethers, and to calculate vibrational frequencies and rotational moments. Other alkali metal ions were not modeled because PM3 parameters for them were not available in SPARTAN.

Radiative association was modeled using the STHYDRO programs provided by Professor Rob Dunbar. Required input parameters include the number of degrees of freedom of the complex, the masses of the ionic and neutral fragments, charge, temperature (assumed to be 298 K), and the polarizability of the neutral (calculated using the atomic hybrid components method [20,21]).

Data treatment: Scheme 1. describes the set of

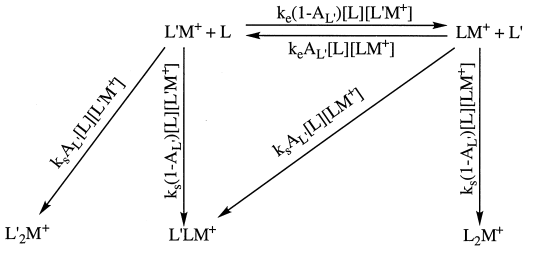

Scheme 1.

reactions used to analyze the kinetics of reaction between a labeled metal-ligand complex and neutral ligands containing ^{13}C at natural abundance. We assume the rate constant for ligand exchange, k_e, is not influenced by kinetic isotope effects. We further assume that the "sandwich" complexes consisting of two ligands bound to the metal do not undergo ligand exchange at an appreciable rate (the experimental results confirm this assumption). The rate constant for formation of sandwich complexes is k_s, isotopic labeling of the ligand L is indicated by L′, and the fractional natural abundance of ^{13}C in the ligand is indicated by $A_{L'}$. Ion populations, measured as FTICR signal intensities, are indicated by symbols in brackets, whereas [L] indicates the partial pressure of the neutral ligand. In practice, L'_2M^+ was not observed in any of the experiments, so it was not considered in the analysis.

The reaction scheme leads to the following coupled set of differential equations, which was solved numerically via the Adams algorithm; the experimental results were then fit to this numerical solution with k_e and k_s as fitting parameters, using the KINFIT Microsoft Excel macros developed in our laboratories.

$$\frac{d[LM^+]}{dt} = k_e[L]\{(1-A_{L'})[L'M^+] - A_{L'}[LM^+]\} - k_s[L][LM^+]$$

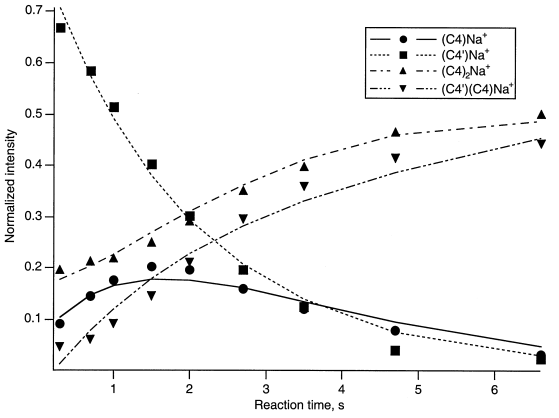

Fig. 1. Ion intensities as a function of time for the reaction of the ^{13}C-labeled C4 complex of Na with natural isotopic abundance C4 ligand. The solid symbols represent experimental data, while the lines are from fits to the data using the set of differential equations resulting from Scheme 1.

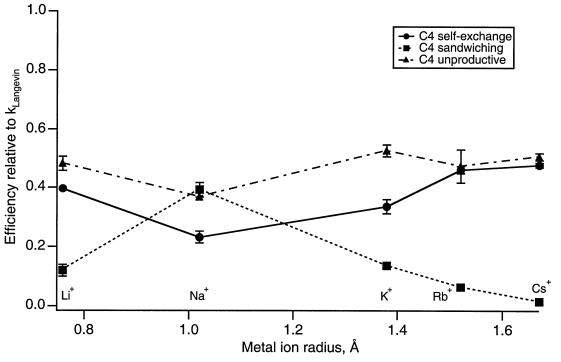

Fig. 2. Efficiencies, relative to the Langevin collision rate, of self-exchange (solid circles) and sandwiching (solid squares) reactions of C4M$^+$, M = alkali metal. The difference between the Langevin collision rate and the sum of self-exchange plus sandwiching rates is also shown (solid triangles), representing the efficiency of complex dissociation back to reactants. Error bars represent one standard deviation for replicate data sets.

$$\frac{d[\mathrm{L'M^+}]}{dt} = k_e[\mathrm{L}]\{A_{\mathrm{L'}}[\mathrm{LM^+}]-(1-A_{\mathrm{L'}})[\mathrm{L'M^+}]\} - k_s[\mathrm{L}][\mathrm{L'M^+}]$$

$$\frac{d[\mathrm{L_2M^+}]}{dt} = k_s(1-A_{\mathrm{L'}})[\mathrm{L}][\mathrm{LM^+}]$$

$$\frac{d[\mathrm{L'LM^+}]}{dt} = k_s[\mathrm{L}]\{(1\text{-}A_{\mathrm{L'}})[\mathrm{L'M^+}]+A_{\mathrm{L'}}[\mathrm{LM^+}]\}$$

3. Results

Figure 1 shows normalized peak intensities as a function of time for a typical self-exchange experiment, this one involving reaction of labeled (C4)Na$^+$ with neutral C4 having natural abundance ^{13}C. From such data, rate constants (Table 1) were extracted by solving the differential equations listed previously and fitting the data to the solutions. Both self-exchange and sandwich products (two crowns adducted to one ion) [6] were observed for all crowns except C7.

The efficiencies (relative to the Langevin collision rate) of self-exchange, sandwich formation, and unproductive reaction (back to reactants) for C4 with the various alkali cations are shown in Fig. 2. The corresponding rate constants are listed in Table 1. The "unproductive reaction" efficiencies are calculated as

Table 1
Rate constants for self-exchange and sandwich formation[a]

	TG		C4		C5		C6		C7	
	Exchange	Sandwich	Exchange	Sandwich	Exchange	Sandwich	Exchange	Sandwich	Exchange	Sandwich
Li^+	5.0 ± 0.1	0.05 ± 0.05	4.1 ± 0.1	1.2 ± 0.2	6.1 ± 0.7	0.04 ± 0.06	11.0 ± 1.1	···[b]	9.3 ± 0.2	···
Na^+	4.6 ± 0.1	0.6 ± 0.06	2.4 ± 0.2	4.0 ± 0.2	5.4 ± 0.9	0.3 ± 0.04	9.0 ± 0.7	···	8.3 ± 0.3	···
K^+	4.5 ± 0.1	0.7 ± 0.02	3.4 ± 0.2	1.3 ± 0.1	4.8 ± 0.9	3.0 ± 0.5	8.7 ± 0.1	···	9.3 ± 0.3	···
Rb^+	5.0 ± 0.1	0.4 ± 0.02	4.4 ± 0.1	0.6 ± 0.1	3.5 ± 0.6	1.8 ± 0.1	7.6 ± 0.8	···	6.9 ± 0.3	···
Cs^+	11.0 ± 0.2	0.02 ± 0.04	4.4 ± 0.1	0.1 ± 0.01	4.5 ± 1.4	0.8 ± 0.1	6.7 ± 0.6	0.4 ± 0.06	8.0 ± 0.6	···

[a] All values $\times 10^{-10}$ cm^3 molecules^{-1} s^{-1}. Error bars represent one standard deviation for three or more replicate measurements.
[b] Reaction not observed.

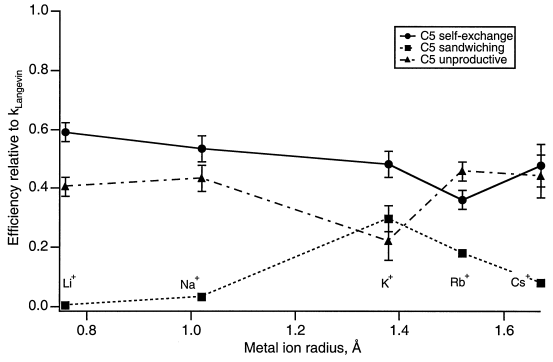

Fig. 3. Efficiencies, relative to the Langevin collision rate, of self-exchange (solid circles) and sandwiching (solid squares) reactions of $C5M^+$, M = alkali metal. The difference between the Langevin collision rate and the sum of self-exchange plus sandwiching rates is also shown (solid triangles), representing the efficiency of complex dissociation back to reactants. Error bars represent one standard deviation for replicate data sets.

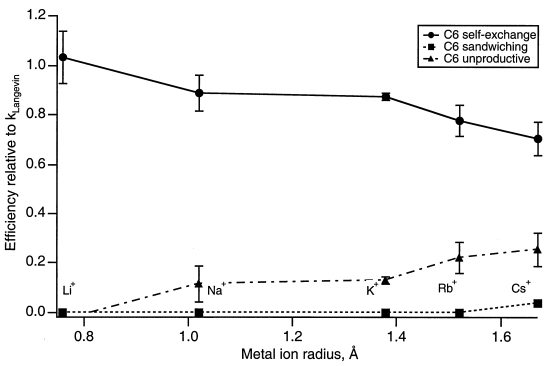

Fig. 4. Efficiencies, relative to the Langevin collision rate, of self-exchange (solid circles) and sandwiching (solid squares) reactions of $C6M^+$, M = alkali metal. The difference between the Langevin collision rate and the sum of self-exchange plus sandwiching rates is also shown (solid triangles), representing the efficiency of complex dissociation back to reactants. Error bars represent one standard deviation for replicate data sets.

$(k_{\text{Langevin}} - k_{\text{self-exchange}} - k_{\text{sandwich}})/k_{\text{Langevin}}$, and so may include considerable absolute error especially because the Langevin collision rate tends to underestimate the true collision rate [22]. In this system, the self-exchange and sandwiching rates are roughly complementary, with the slowest self-exchange and fastest sandwiching occurring for Na^+, so the efficiency of unproductive dissociation to reactants is roughly constant as the metals vary. It is interesting to note that ligand exchange processes for the sandwich complexes were observed to have negligible rates in all cases examined.

Fig. 3 shows the efficiencies for the self-reactions of C5 complexes. The self-exchange efficiencies decrease gradually from Li^+ through Rb^+, and probably through Cs^+, although the relative error for the latter is large. In agreement with prior measurements [3,6], the sandwiching efficiencies for C5 complexes peak with K^+, in apparent competition with dissociation to reactants.

For C6 (Fig. 4) and C7 (Fig. 5), the self-exchange reaction dominates for each alkali cation, and sandwiching is observed only for $(C6)Cs^+$ and then only at about 5% efficiency. Again, this is in good agreement with earlier measurements of sandwiching efficiencies [3,6]. The self-exchange efficiencies reported here are probably too high, because even complete scrambling of the C6 ligands should result in self-exchange efficiencies no greater than 50% as the labeled and unlabeled ligands become equivalent. Again, this probably is a result of underestimation of the collision rate and possibly of errors in the measurement of the neutral pressure.

Fig. 6 reports results for the acyclic analog of C4, triglyme (TG). In contrast with C4, and in agreement with earlier results [3,6], the sandwiching efficiencies

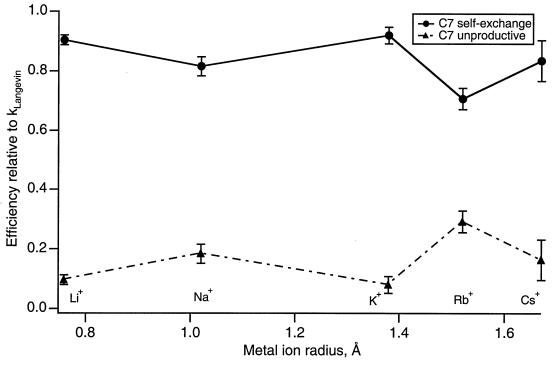

Fig. 5. Efficiencies, relative to the Langevin collision rate, of self-exchange (solid circles) and sandwiching (solid squares) reactions of $C7M^+$, M = alkali metal. The difference between the Langevin collision rate and the sum of self-exchange plus sandwiching rates is also shown (solid triangles), representing the efficiency of complex dissociation back to reactants. Error bars represent one standard deviation for replicate data sets.

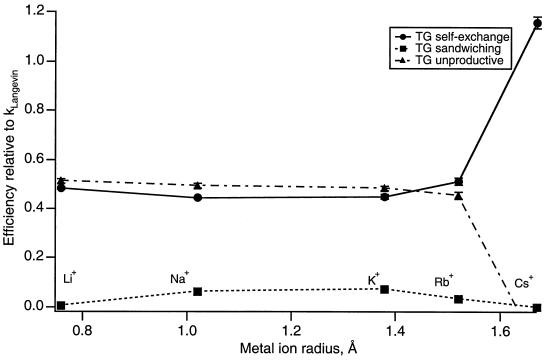

Fig. 6. Efficiencies, relative to the Langevin collision rate, of self-exchange (solid circles) and sandwiching (solid squares) reactions of TGM^+, M = alkali metal. The difference between the Langevin collision rate and the sum of self-exchange plus sandwiching rates is also shown (solid triangles), representing the efficiency of complex dissociation back to reactants. Error bars represent one standard deviation for replicate data sets.

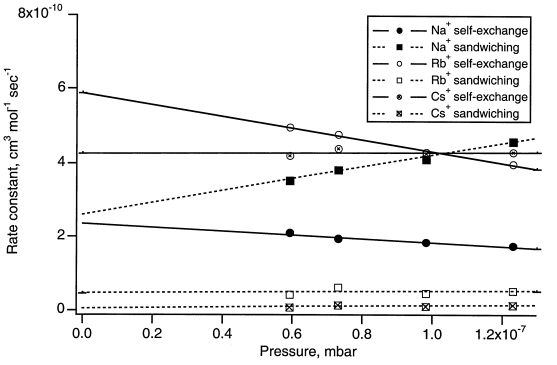

Fig. 7. Effects of added N_2 pressure on the rates of self-exchange (circles with solid lines) and sandwiching (squares with dotted lines) for Na^+, Rb^+, and Cs^+ complexes of C4. The lines represent linear least-squares fits to the data.

are less than 10% for each metal ion. While the greatest sandwiching efficiencies are observed for K^+, they do not peak strongly; the Na^+ and Rb^+ complexes have similar sandwiching efficiencies. The self-exchange efficiencies, on the other hand, are all around 50% for Li^+–Rb^+,and exchange occurs approximately at the Langevin collision rate for the Cs^+ complex. Accordingly, dissociation back to reactants has about the same efficiency as self-exchange for the Li^+–Rb^+ complexes, and is negligible for the Cs^+ complex. We currently have no definitive explanation for the anomalous behavior of the Cs^+ complex, but note that the bond strengths are probably very low for this combination of ligand and metal.

Fig. 7 shows self-exchange and sandwiching rate constants of C4 complexes as a function of background N_2 pressure. The N_2 serves as an inert collision partner. Extrapolation of the rate constants to the zero pressure limits allows examination of the reactions under collisionless conditions, because third-body collisional stabilization becomes negligible at low pressures. This facilitates examination of unimolecular and radiative association processes [23]. Table 2 summarizes the slope and zero pressure limits for the self-exchange and sandwich formation rates of Na, Rb, and Cs ions with C4 shown in Fig. 7. In general, self-exchange rates decrease with increasing pressure, while sandwich complex formation rates increase, reflecting increased collisional stabilization of the nascent sandwich collision complex.

Minimum-energy conformers located with the AMBER conformational searches are pictured in Figs. 8 and 9 in space-filling and tube representations, respectively. Several trends are apparent in the modeling results. For C4, and to a lesser extent for C5, complexes of the small cations have a “sandwichlike” structure, wherein the mean planes of the atoms of each ligand are approximately parallel. As the size of the metal increases, the ligands are forced apart and the ligand planes become increasingly nonparallel, reflecting the propensity of the polyether ligands to simultaneously coordinate the metal and achieve optimal van der Waals contact with each other. The relatively large cavity of C6 leads to different trends in its L_2M^+ complexes. The C6 cavity is large enough that in complexes of the smaller cations, Li^+, Na^+, and to a lesser extent, K^+, the metal is largely encapsulated by one of the ligands, while the other ligand is attached to the metal by only two or three oxygen atoms. Thus, these complexes are highly asymmetric (and none of these are experimentally observed). The Rb^+ and Cs^+ complexes involve roughly equal binding of the metal by both ligands; similar to the situation observed for the smaller crowns binding Li^+ and Na^+.

Two binding motifs are observed in the minimum

Table 2
Rate constants and slopes for variable pressure experiments[a]

Reaction	Slope ($\times 10^{-4}$ cm^3 molecules^{-1} s^{-1} mbar^{-1})	Zero pressure limit rate constant ($\times 10^{-10}$ cm^3 molecules^{-1} s^{-1})
$Na(C4)^+$ self-exchange	-5.1 ± 0.8	2.3 ± 0.1
$Na(C4)_2^+$ formation	16.0 ± 1.2	2.6 ± 0.1
$Rb(C4)^+$ self-exchange	-15.8 ± 1.0	5.9 ± 0.1
$Rb(C4)_2^+$ formation	0.4 ± 2.4	0.5 ± 0.2
$Cs(C4)^+$ self-exchange	0.2 ± 1.9	4.2 ± 0.2
$Cs(C4)_2^+$ formation	0.7 ± 0.6	0.04 ± 0.05

[a] Error estimates are standard deviations for slope and intercept from least-squares analysis.

energy structures of the L_2M^+ complexes of TG. For the smaller cations, Li^+ and Na^+, the TG complexes are very similar to those of C4 or C5: one ligand lies on either side of the metal, in a sandwichlike structure with the mean planes of the ligands parallel. For the larger alkali cations, but most obviously for K^+, the mean planes of the two ligands are orthogonal, forming a structure with symmetry similar to that of the cover of a baseball. As the metals become larger, especially for Cs^+, the structure becomes distorted and coverage of the metal by the ligand is less complete.

4. Discussion

4.1. Trends in self-exchange versus sandwich formation

Figs. 8 and 9 show AMBER* force field [24] molecular mechanics models of complexes of the alkali metal ions with C4. "Size matching" has been used previously to explain metal complexation affinities [2,25]. This terminology usually refers to the match between ligand cavity size and ion radius. Researchers have also seen size effects in 1:2 complexation in the gas phase, where the fastest rates of

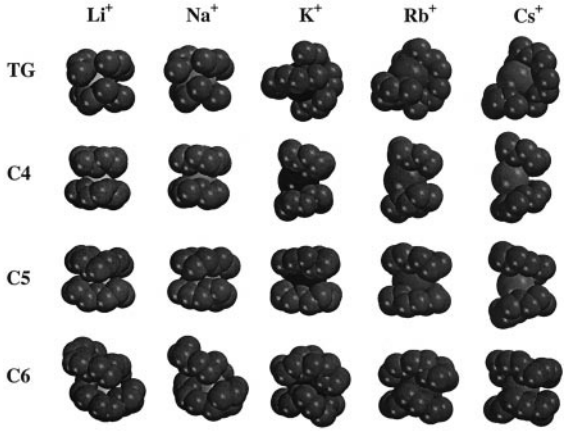

Fig. 8. Space-filling representations of minimum-energy structures from Monte Carlo conformational searches using the AMBER force field for L_2M^+ complexes, L = C4, C5, or C6; M = Li, Na, K, Rb, or Cs. Hydrogen atoms removed for clarity.

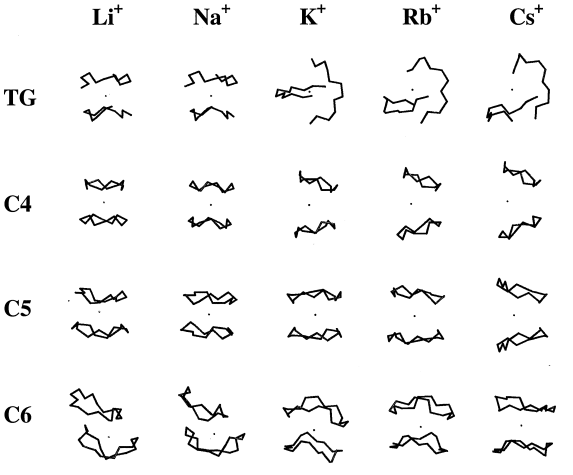

Fig. 9. Tube representations of minimum-energy structures from Monte Carlo conformational searches using the AMBER force field for L_2M^+ complexes, L = C4, C5, or C6; M = Li, Na, K, Rb, or Cs. Hydrogen atoms removed for clarity. The orientation of the models is the same as in Fig. 8.

sandwich formation for each crown ether studied are for the complexes $Na(C4)_2^+$, $K(C5)_2^+$, $Cs(C6)_2^+$, and no sandwich formation was observed for C7 [4,6]. The best explanation is perhaps the correlation between the ion radius and the cavity radius of the pocket formed by two crowns sandwiched together as closely as steric hindrances allow. The ion can be considered nested in both of the crowns.

There are three general cases when considering size matching. The first case, an example of which is the $Li(C6)_2^+$ complex (Figs. 8 and 9), is one in which the metal is too small to be nested equally in both crowns, and is therefore drawn into one of the crown cavities at the expense of the other. This is the most general case, especially for C6 and C7. The second case occurs when the crowns are separated from one another by the metal ion and the ion is so large it cannot be accommodated into the cavity of either crown even with extensive ligand conformational rearrangement. This occurs mainly for combinations of the larger metals with the smaller ligands. The third and rarest case arises when the metal is well nested in both crowns equally without extensive steric hindrance between the ligands. The modeling results suggest this is the case for $Na(C4)_2^+$, $K(C5)_2^+$, and $Rb(C6)_2^+$. The ratio of ion radius to cavity radius for these species is similar, around 1.5:1. It is interesting to note in Figs. 2, 3, and 4 that these species involve the highest total (self-exchange plus sandwich formation) reaction efficiencies of any of the alkali cation complexes of C4, C5, and C6, respectively.

For case one, in order for self-exchange to occur, the reaction must proceed through a barrier because bonds with the donor atoms of one crown must be broken to allow bond formation with donor atoms of the other. The transition state for this exchange, in the most simplistic view, is a midpoint where the ion is equidistant from the donor oxygen atoms of one crown and those of the other. The barrier disappears for larger metal ions (case two), because the ion is already equidistant between the two ligands in the lowest energy configuration. If the barrier to self-exchange were large enough for case one systems (highly asymmetric complexes), we would expect to see a decrease in the self-exchange rates compared to those for species where the ion is more symmetrically bound by the ligands. Experimentally, the reverse is true: the more asymmetric complexes tend to have faster self-exchange rates (see Fig. 3 for the C5 complexes, and Fig. 4 for the C6 complexes, for example). This suggests that collision complex lifetimes are long enough for the asymmetric systems that the barrier, whatever its magnitude, is crossed repeatedly during the lifetime of the collision complex.

A complication to the analysis of self-exchange rates is the competition between self-exchange and sandwich formation. The sandwich structures shown in Fig. 8 and Fig. 9 are the products of a collisionally or radiatively stabilized collision complex, and as such can be considered self-exchange products that failed to dissociate into complex ion and neutral crown. Sandwich formation and redissociation both compete with self-exchange. Therefore, longer collision complex lifetimes should lead to increased opportunity for collisional or radiative stabilization, and hence larger branching ratios in favor of sandwich complex formation.

Arguments can be made for both the larger and the smaller crowns to have the longest collision complex lifetimes. Because the larger complexes have more degrees of freedom, and more donor atoms leading to greater total binding, we would expect the lifetime of the larger collision complexes to be longer and therefore the rate of sandwich formation to be greater for large crowns than for small ones. However, for asymmetric crown-metal complexes, it is likely that binding for the second ligand becomes weaker as the crowns become larger, because the first crown fills the coordination sphere of the metal leaving little purchase for a second ligand. Indeed, radiative association kinetic determination of the binding strengths (vide infra) shows binding energies decrease for Li^+ complexes as the size of the crown in the complex increases. Though there are more degrees of freedom in the large crown systems, there are also more low frequency vibrational modes (the number of vibrational modes in the activated complex with frequencies 50 cm^{-1} or less is 6 for C4, 6 for C5, 9 for C6, and 11 for C7 based on the PM3 calculations). It has been proposed that these low frequency modes are the

most important for dissociation kinetics, because these modes correspond to torsions, bending, and other hindered motion that is released as the complex dissociates. The more modes, the larger the statistical driving force to dissociation [26]. We conclude then that the C6 and C7 collision complexes would actually dissociate most rapidly, whereas C4 and C5 would yield the longest-lived collision complexes. This conclusion is in keeping with experiment, where C4 and C5 have the largest sandwich formation rates, and C6 and C7 have very slow rates of sandwich formation.

The prior explanation for trends in sandwich formation rates is seemingly inconsistent with the trends observed for self-exchange. We argued above that larger sandwich complexes have shorter lifetimes, which would lead to the conclusion that self-exchange should be slower for the larger crowns. However, the situation for self-exchange is not as simple as that for sandwich formation, where the formation rate is a competition between stabilization and dissociation. The self-exchange rate depends on the statistics of dissociation and on the difference between the heights of the barriers to self-exchange and to dissociation.

Statistical factors may be part of the explanation for the finding that self-exchange is more efficient for the larger crowns than for the smaller crowns. In the case of $(C7)M^+$, none of the metals match the ligand cavity size well, and the smaller metals are likely to be coordinated to only a few of the oxygen donors. The number of ways the metal can move from the labeled to the unlabeled crown is larger for C7 than for C4, because the number of oxygen atoms that can participate is larger for C7, and thus there is a higher number of (nearly) degenerate transition states for C7 than for C4. Evidence for the importance of the statistical factor can be seen in the trends for the general decrease in self-exchange rate efficiencies as the metal size increases (Fig. 3, and Fig. 4, for C5 and C6, respectively) because more oxygen atoms are involved in binding as the metal gets bigger, and thus the degeneracy decreases.

Another factor that must be considered is the height of the barrier to self-exchange, which is related to the strengths of the bonds between the metal and the two ligating crowns. Equilibrium studies show that transfers of metal from a 1:1 crown complex to another, different crown, proceed from the smallest to the largest crown in every case [6], indicating that overall binding energies are largest for larger crowns. However, *individual* oxygen–metal bonds are weaker for the larger crowns than for smaller ones. For example, bond dissociation enthalpies of multiple dimethyl ether (DME) complexes with Li^+ show that the higher the number of DMEs coordinated to Li^+, the lower the bond dissociation enthalpy for removal of one of the DMEs: D_{298} (Li^+–DME) = 167 kJ/mol, D_{298} ($Li(DME)_3^+$–DME) = 66 kJ/mol [27]. Thus the average energy required for removal of a single DME *decreases* with increased coordination.

An analogous experiment compared bond dissociation enthalpies for $Li(C4)^+$ and $Li(DXE)_x^+$, where DXE = dimethoxyethane ($CH_3O(CH_2)_2OCH_3$), and x = 1 and 2. The results showed that the total bond dissociation enthalpy for $Li(DXE)_2^+$ is roughly equivalent to that of $Li(C4)^+$, but that the bond dissociation enthalpy for removal of DXE from $Li(DXE)_2^+$ is roughly half that of the bond dissociation enthalpy for removal of DXE from $Li(DXE)^+$ [28]. If the bonds between Li^+ and C4 are broken stepwise, we expect a much lower enthalpic price would have to be paid for the first metal–oxygen bond, and that each consecutive cleavage would have a higher energetic cost.

A simplistic view of the reaction coordinate is the movement of the metal ion from the cavity of one crown to another, with simultaneous bond cleavage from the "donor" crown and bond formation with the "receiver" crown. Of all the crowns in this study, C4 would most closely fit this model, because the ligand is relatively rigid and the oxygen–metal binding would therefore be cooperative. In contrast, C6 or C7, which are not conformationally rigid, can more easily rearrange, and one or two oxygen–metal bonds could be broken without cleavage of the other bonds of the complex. Self-exchange could then proceed more stepwise, with one or two reactant crown oxygen atoms being replaced by product crown oxygen atoms at a time. After removal of the first reactant crown oxygen atoms, the subsequent oxygen atoms would have similar bond strengths, since the coordination

number would remain roughly constant because of coordination of receiver crown oxygen atoms. This "stepwise" self-exchange would have a much lower barrier than would processes invoking simultaneous cleavage of all donor crown–metal bonds. The larger crowns would have smaller exchange barriers because they could more easily exchange one or two oxygen atoms at a time, in contrast to the more rigid smaller crowns, and because their individual metal–oxygen bond strengths are smaller. Thus, self-exchange could be faster for the larger ligands because the process can proceed in a more stepwise fashion. Similar arguments have been used to rationalize the kinetics of crown exchange on divalent alkaline earth cations [29].

The comparison between cyclic C4 (Fig. 2) and acyclic TG (Fig. 6) is interesting. For both ligands, the sum of the self-exchange and sandwich formation rate constants is in the same general range, but what differs is the branching ratio between sandwich formation and self-exchange. Triglyme greatly favors self-exchange over sandwich formation, and its rate of self-exchange is much larger than that of C4. One plausible explanation is that the collision complex lifetime is greater for C4, resulting in greater sandwich complex stabilization. Such would be the case if the ML^+–L bond energy is significantly less for L = triglyme than for L = C4. This would not be surprising in light of the relative flexibility of the two ligands. Triglyme is sufficiently flexible that the first ligand to attach mostly satisfies the coordination requirements of the metal, leaving less opportunity for a second ligand to bind well. C4 lacks the ability to place its donor groups optimally, leaving a greater coordinative "opportunity" for the second ligand. The relatively large reaction rate for $Cs(TG)^+$ self-exchange could be due to thermal dissociation of $Cs(TG)^+$ into Cs^+ and TG, followed by subsequent statistical complex formation. This hypothesis will be tested in future experiments.

Comparison of the self-exchange rates of C4 and TG also supports our ideas about the step-wise nature of the exchange mechanism. Self-exchange rates for TG are greater than those of C4 for all the metals, despite the fact that the total M^+–L bond strength is believed to be greater for L = TG. Because TG is much more flexible than C4, it is easier to break individual M^+–O bonds in the TG complex than in complexes with the more rigid C4. In the latter, it is likely that bond breaking involves multiple coordinated M^+–O cleavages, for which the activation barrier is higher and rates are slower.

4.2. Reaction efficiencies

Self-exchange rates for C6 and C7 have measured efficiencies close to 1. This is statistically unreasonable, because complete scrambling of the metal ion between the crowns should give a maximum efficiency of 0.5. Most likely, our efficiencies are overestimated because the collision rate is underestimated. Langevin theory, used to estimate the collision rates, is known to give results that are significantly low [22]. The systems studied here are likely further complicated by dipole–induced-dipole interactions, since the ion in our case is a cation with one highly polarizable crown already complexed to it. The dipole of the neutral crown can induce a dipole on the one complexed with the metal cation, and would result in a larger collision rate than that predicted by either Langevin or ADO theory [22,30,31]. If we assume that the $Li(C6)^+$ self-exchange rate (the fastest observed reaction rate) proceeds at one-half the collision rate, we can estimate that Langevin theory underestimates the collision rate by a factor of 2, which is not unreasonable. ADO efficiencies (using dipoles from PM3) are closer to the fastest observed self-exchange rate, but are still low by a factor of around 1.5.

4.3. Radiative association kinetic estimation of bond strengths

Dunbar [14,23,32,33] has recently demonstrated the intimate connection between the kinetics of radiatively stabilized complex formation and the strength of the bond being formed, and has developed methods for extracting bond strengths from rate constants for radiative association processes. Radiative association kinetic analysis is most successful in cases where the observed reactions have low efficiencies, as is the case for most of the sandwich complex formation

Table 3
Bond dissociation energy estimates (kJ mol^{-1}) from radiative association kinetic analysis with the standard hydrocarbon model[a]

	TG	C4		C5		C6	
	$D(LM^+-L)$[b]	$D(M^+-L)$[c]	$D(LM^+-L)$	$D(M^+-L)$[c]	$D(LM^+-L)$	$D(M^+-L)$[c]	$D(LM^+-L)$
Li	108	. . .[d]	135	. . .	104	. . .	<94[e]
Na	127	254 ± 13, 258	150, 144[f]	298 ± 18, 324	118	300 ± 19, 336	<94
K	128	191 ± 11, 196	135	206 ± 14, 248	138	235 ± 13, 299	<94
Rb	123	95 ± 13, 164	129, 128[f]	116 ± 6, 208	133	192 ± 13, 243	<94
Cs	102	86 ± 9, 140	118, 110[f]	101 ± 6, 179	125	170 ± 9, 204	120

[a] All values at 298 K.
[b] This work. Estimated error is ±10 kJ mol^{-1}.
[c] Values from [34]. The first value in each case is an experimental value from threshold collision-induced dissociation measurements, whereas the second is from MP2 level computational results.
[d] No values reported.
[e] Complex formation was not observed. An upper limit to the binding enthalpy was estimated by assuming the complexation rate constant was less than 1×10^{-12} cm^3 $molecules^{-1}$.
[f] Value obtained after extrapolating formation rate to zero pressure limit.

reactions. We have therefore employed Dunbar's methods to estimate $D(ML^+–L)$.

Specifically, we used Dunbar's standard hydrocarbon model to describe the radiative and unimolecular dissociation rates of the nascent sandwich complexes, allowing estimation of the bonding enthalpies. The results are given in Table 3. We note that rigorous treatment of the data requires the use of rate constants for pure radiatively stabilized processes, and as demonstrated in Table 2, sandwich complex formation at the pressures used in our experiments exhibits a small pressure dependence and therefore is both collisionally and radiatively stabilized. For a few cases, we have extrapolated the complex formation rate constants to the zero pressure limits to obtain values for purely radiative complex stabilization. Application of the pressure correction decreases the estimated bonding enthalpies by 1–8 kJ mol^{-1}. Given the magnitude of the other errors involved in these estimates, we have chosen to report values without making the pressure correction in most cases.

Although $D(M^+–L)$ decreases monotonically with increasing alkali cation size for a given ligand [34], selective size effects are clearly evident in the bond enthalpy trends for attachment of a second ligand (Table 3). For example, the enthalpy for attachment of a second TG is small for Li^+, peaks for Na^+ and K^+, then falls off again for Rb^+ and Cs^+. Similarly, for L = C4 $D(LM^+–L)$ is greatest for M = Na^+, whereas for C5 it is greatest for M = K^+. These trends likely reflect the ability of the first ligand to occupy the inner coordination space of the metal. For small metals, the first ligand encapsulates the metal, decreasing the ability of the second ligand to bind effectively. Thus, second ligand binding enthalpies are often smaller for the small metals, despite the intrinsically greater polarizing ability of small, charge-dense cations, and the effects are more apparent as the ligands become larger. Similarly, flexible, acyclic ligands (such as TG) encapsulate the metals more effectively than more rigid, cyclic ligands (such as C4), so $D(LM^+–L)$ is always less for L = TG than for L = C4.

Comparison of $D(M^+–L)$ (from the collision-induced dissociation measurements of Armentrout) [34] and $D(LM^+–L)$ generally shows the expected result that $D(M^+–L) > D(LM^+–L)$. As with the alkali cation complexes of dimethyl ether and dimethoxyethane [27,28,34–37], polarization of the cation and steric factors contribute to decrease the total binding strength as additional ligands are added. The cases where $D(M^+–L) < D(LM^+–L)$ involve Rb^+ and Cs^+ complexes of C4 and C5, where the CID results are in poor agreement with high-level computational results. It has been proposed that these CID

results do not reflect dissociation of complexes from the global conformational minimum energy structures, but from higher-energy conformers produced via ion–molecule reactions and separated from the global minima by energetic barriers [34]. If the MP2 results are taken to be the correct values for the global minimum energy conformers, then in all cases $D(M^+–L) > D(LM^+–L)$, as expected.

5. Conclusions

The self-exchange experiment provides a unique look at reaction dynamics, since it allows us to observe products that were previously unobservable. As was seen in the discussion of the branching ratio of sandwich formation and self-exchange, the results are complementary to previous results and help to shed new light on unimolecular decomposition of multidentate ligands.

For a given ligand, self-exchange rates generally decrease with increasing metal size, probably reflecting the decreasing strength of individual metal–oxygen interactions as the metals become larger and more diffuse. For a given metal, the self-exchange rates generally increase as ligand size increases. The reasons for this trend are not clear, but statistical factors likely play a role as there are more ways to effect ligand exchange for larger ligands than for smaller ones. In addition, because they are more flexible the larger ligands are more likely to exchange by stepwise processes with low barriers than the smaller ligands, which are more rigid and therefore more likely to exchange by more concerted, higher energy processes. The self-exchange reactions have weak, negative pressure dependences, suggesting they are in direct competition with sandwich complex formation.

Sandwich complex formation rates show strong dependence on the relative sizes of the metal ions and ligand cavities. These trends can be rationalized in terms of competition between the two attached ligands for the metal coordination sites, with weak binding of the second ligand when the size of the first is appropriate for encapsulating the metal. Estimation of the ligand binding enthalpies using radiative association kinetic analysis supports this explanation. Sandwich formation rates show a weak positive pressure dependence, as increased pressure leads to increased collisional stabilization of the complexes. Extrapolation to the zero pressure limits still yields significant rates, suggesting the reactions are radiatively stabilized.

Acyclic TG complexes undergo self-exchange more rapidly than the analogous cyclic C4 complexes, whereas the sandwich complex formation rates are faster for the C4 complexes. Again, this is consistent with a stepwise mechanism for self-exchange: the acyclic ligand is more flexible and therefore can more easily exchange one donor atom at a time, whereas the cyclic ligand is restricted by the ligand framework into more concerted exchange processes. Sandwich formation is faster for the crowns most likely because a second crown binds the metal with greater enthalpy than does a second glyme, leading to greater collision complex lifetimes and greater chance for stabilization for the crown complex.

Analysis of the sandwich complex formation radiative association kinetics yields estimates of binding enthalpies for attachment of the second ligand. Trends in the binding enthalpies, like the kinetics, show strong dependence on the relative sizes of the metal ions and ligand cavities. For a given metal, binding of a second TG is weaker than binding of a second C4. Binding enthalpies for the second ligand are in every case substantially less than calculated binding enthalpies for the first ligand to attach to a given metal.

Acknowledgements

The authors are grateful for support of this work by the donors of the Petroleum Research Fund, administered by the American Chemical Society, and the National Science Foundation. They would also like to thank Professor Rob Dunbar for making his STHYDRO program available.

References

[1] C.A. Schalley, Int. J. Mass Spectrom. 194 (2000) 11.

[2] R.M. Izatt, K. Pawlak, J.S. Bradshaw, R.L. Bruening, Chem. Rev. 91 (1991) 1721.
[3] H. Zhang, I.-H. Chu, S. Leming, D.V. Dearden, J. Am. Chem. Soc. 113 (1991) 7415.
[4] H. Zhang, D.V. Dearden, J. Am. Chem. Soc. 114 (1992) 2754.
[5] D.V. Dearden, H. Zhang, I.-H. Chu, P. Wong, Q. Chen, Pure Appl. Chem. 65 (1993) 423.
[6] I.H. Chu, H. Zhang, D.V. Dearden, J. Am. Chem. Soc. 115 (1993) 5736.
[7] S. Maleknia, J. Brodbelt, Rapid Commun. Mass Spectrom. 6 (1992) 376.
[8] S. Maleknia, J. Brodbelt, J. Am. Chem. Soc. 114 (1992) 4295.
[9] C.C. Liou, J.S. Brodbelt, J. Am. Soc. Mass Spectrom. 3 (1992) 543.
[10] H.-F. Wu, J.S. Brodbelt, J. Am. Chem. Soc. 116 (1994) 6418.
[11] I.-H. Chu, D.V. Dearden, J. Am. Chem. Soc. 117 (1995) 8197.
[12] Q. Chen, K. Cannell, J. Nicoll, D.V. Dearden, J. Am. Chem. Soc. 118 (1996) 6335.
[13] A.G. Marshall, F.R. Verdun, Fourier Transforms in NMR, Optical, and Mass Spectrometry: A User's Handbook, Elsevier, Amsterdam, 1990.
[14] R.C. Dunbar, Int. J. Mass Spectrom. Ion Processes 160 (1997) 1.
[15] L. Chen, T.-C.L. Wang, T.L. Ricca, A.G. Marshall, Anal. Chem. 59 (1987) 449.
[16] A.J.R. Heck, L.J. de Koning, F.A. Pinkse, N.M.M. Nibbering, Rapid Commun. Mass Spectrom. 5 (1991) 406.
[17] F. He, A.G. Marshall, J. Phys. Chem. A 104 (2000) 562.
[18] J.J.P. Stewart, J. Comput. Chem. 10 (1989) 209.
[19] J.J.P. Stewart, J. Comput. Chem. 10 (1989) 221.
[20] K.J. Miller, J.A. Savchik, J. Am. Chem. Soc. 101 (1979) 7206.
[21] K.J. Miller, J. Am. Chem. Soc. 112 (1990) 8533.
[22] T. Su, M.T. Bowers, Classical Ion–molecule Collision Theory, M.T. Bowers (Ed.), Gas Phase Ion Chemistry Vol. 1, Academic, New York, 1979, p. 83.
[23] V. Ryzhov, S.J. Klippenstein, R.C. Dunbar, J. Am. Chem. Soc. 118 (1996) 5462.
[24] S.J. Weiner, P.A. Kollman, D.T. Nguyen, D.A. Case, J. Comput. Chem. 7 (1986) 230.
[25] R.M. Izatt, J.H. Rytting, D.P. Nelson, B.L. Haymore, J.J. Christensen, Science 164 (1969) 443.
[26] B. McNamara, M.H. Towns, E.R. Grant, J. Am. Chem. Soc. 117 (1995) 12254.
[27] M.B. More, E.D. Glendening, D. Ray, D. Feller, P.B. Armentrout, J. Phys. Chem. 100 (1996) 1605.
[28] D. Ray, D. Feller, M.B. More, E.D. Glendening, P.B. Armentrout, J. Phys. Chem. 100 (1996) 16116.
[29] N. Shen, R.M. Pope, D.V. Dearden, Int. J. Mass Spectrom. 195–196 (2000) 639.
[30] C. Praxmarer, A. Hansel, W. Lindinger, J. Chem. Phys. 100 (1994) 8884.
[31] C. Praxmarer, A. Hansel, W. Lindinger, Int. J. Mass Spectrom. Ion Processes 156 (1996) 189.
[32] R.C. Dunbar, S.J. Klippenstein, J. Hrusák, D. Stöckigt, H. Schwarz, J. Am. Chem. Soc. 118 (1996) 5277.
[33] V. Ryzhov, R.C. Dunbar, Int. J. Mass Spectrom. Ion Processes 167 (1997) 627.
[34] M.B. More, D. Ray, P.B. Armentrout, J. Am. Chem. Soc. 121 (1999) 417.
[35] M.B. More, D. Ray, P.B. Armentrout, J. Phys. Chem. A 101 (1997) 831.
[36] M.B. More, D. Ray, P.B. Armentrout, J. Phys. Chem. A 101 (1997) 7007.
[37] M.B. More, D. Ray, P.B. Armentrout, J. Phys. Chem. A 101 (1997) 4254.